18th Mediterranean Conference on Control & Automation
Congress Palace Hotel, Marrakech, Morocco
June 23-25, 2010

Incorporating smoothness into weight optimization for $\mathscr{H}_\infty$ loop-shaping design

Mobolaji Osinuga, Sourav Patra and Alexander Lanzon

***Abstract*— Smoothness constraints are formulated for weights in $\mathscr{H}_\infty$ loop-shaping design in order to ensure smooth variations in their magnitude response. Smoothness in the magnitude response of weights prevents the cancelation of lightly damped poles/zeros of the plant when the shaped plant is formed by cascading the nominal plant with the weights. It also allows fitting by low-order transfer functions when the smooth variations are computed point-wise in frequency. Gradients of weights, expressed in dB/decade, are used to formulate the smoothness constraints in LMI form as additional constraints to those on the singular values and condition numbers of weights in [Lanzon, 2005, Weight optimization in $\mathscr{H}_\infty$ loop-shaping, Automatica, 41(1): 1018-1029]. The resulting solution algorithm maximizes the robust stability margin while simultaneously synthesizing smooth weights and a stabilizing controller subject to the shaped plant lying within a specified region that depicts the closed-loop design requirements.**

Keywords: $\mathscr{H}_\infty$ loop-shaping; Smoothness constraint; Weight optimization; Robust control.

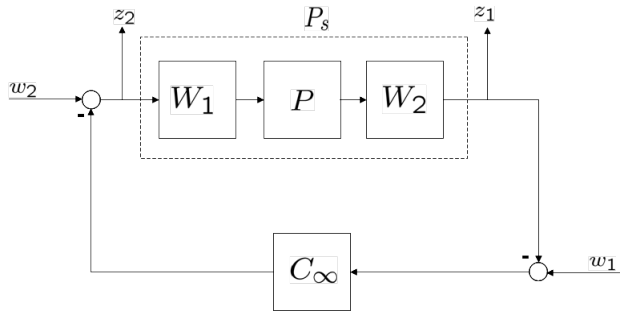

Fig. 1: Feedback interconnection

I. Introduction

A well-known design methodology that combines classical loop-shaping concepts with $\mathscr{H}_\infty$ synthesis is the so-called $\mathscr{H}_\infty$ loop-shaping design procedure (LSDP) [1]. This procedure establishes a good tradeoff between robust performance and robust stability of a closed-loop system in a systematic framework where the closed-loop design objectives are specified in terms of loop-gain of the compensated system. This design framework is depicted in Figure 1 where a stabilizing controller C_∞ is synthesized for the shaped plant $P_s = W_2 P W_1$ and the final $\mathscr{H}_\infty$ loop-shaping controller is obtained by cascading weights with the stabilizing controller C_∞ as $C = W_1 C_\infty W_2$.

The design framework is captured in three steps: (i) W_1 and W_2 are selected such that P_s has the desired loop-shape that satisfies closed-loop specifications, (ii) the optimal robust stability margin $b_{opt}(P_s)$ is estimated once a desired loop-shape is achieved and (iii) C_∞ is then synthesized based on P_s. The achieved robust stability margin indicates the success of the LSDP. Hence, a designer's objective is to select weights that achieve large robust stability margin. It should however be noted that the weight selection process is non-trivial and factors such as right-half plane poles/zeros of the nominal plant, strength of cross-coupling for multi-input multi-output (MIMO) systems, roll-off rate around cross-over, singular values and condition numbers of the loop-shaping weights etc. must be duly considered. All of these factors have been discussed in detail in [1]–[4].

In reducing the length of iterations between the steps of $\mathscr{H}_\infty$ LSDP by eliminating trial and error in Step 1, these factors have been combined in [2] into a single optimization framework that facilitates design via an algorithm that maximizes the robust stability margin while simultaneously synthesizing weights and a stabilizing controller. This algorithm is computationally efficient as the optimization problem is posed in quasiconvex form that is easily implementable using available LMI toolbox to design either diagonal or non-diagonal weights.

In this paper, based on the motivation in Section III, smoothness constraints are formulated in Section IV. A solution algorithm to solve the posed optimization problem is presented in Section V and a numerical example is given in Section VI to elucidate the efficacy of the constraints. The conclusion is given in Section VII. Next, notations that are central to subsequent sections are defined.

II. Notation and definition

Let $\mathbb{R}, \mathbb{R}_+, \mathbb{R}_+^n$ respectively denote the set of real numbers, strictly positive real numbers and column vectors of dimension $(n \times 1)$ with each entry belonging to $\mathbb{R}_+$. $\mathscr{R}^{n\times m}$ and $\mathscr{RH}_\infty^{n\times m}$ are the set of real rational and real rational stable transfer function matrices respectively, each of dimension $(n \times m)$. Functions that are units in $\mathscr{RH}_\infty$ belong to $\mathscr{GH}_\infty$, i.e $f \in \mathscr{GH}_\infty \Leftrightarrow f, f^{-1} \in \mathscr{RH}_\infty$. $\mathrm{diag}\begin{pmatrix} a \\ b \end{pmatrix}$ is a shorthand notation for $\begin{pmatrix} a & 0 \\ 0 & b \end{pmatrix}$. Let $\mathbf{\Lambda_n}$ represent the set of real strictly positive diagonal matrices of dimension $(n \times n)$, defined as $\mathbf{\Lambda_n} := \{\mathrm{diag}(x) : x \in \mathbb{R}_+^n\}$. Also, let $\mathscr{C}(P)$ denote

Control Systems Centre, University of Manchester, Manchester. M60 1QD (mobolaji.osinuga-2@postgrad.manchester.ac.uk). The financial support of the Engineering and Physical Sciences Research Council (EPSRC grant number EP/F06022X/1) and the Royal Society (via a research grant) is gratefully acknowledged.

the set of all stabilizing controllers for a plant P. For matrix A, the i-th singular value is represented as $\sigma_i(A)$ and the condition number is defined as $\kappa(A) := \overline{\sigma}(A)/\underline{\sigma}(A)$, where $\overline{\sigma}(A)$ (resp. $\underline{\sigma}(A)$) is the largest (resp. smallest) singular value. The robust stability margin $b(P_s, C_\infty)$ of the feedback interconnection shown in Figure 1 is defined as

$$b(P_s, C_\infty) := \left\| \begin{bmatrix} P_s \\ I \end{bmatrix} (I - C_\infty P_s)^{-1} \begin{bmatrix} -C_\infty & I \end{bmatrix} \right\|_\infty^{-1}$$

if $C_\infty \in \mathscr{C}(P)$ otherwise 0. The maximum achievable robust stability margin $b_{opt}(P_s) := \sup_{C_\infty} b(P_s, C_\infty) \in [0,1]$. The following two sets are defined for compactness of notation:

$\mathbf{\Xi}(\alpha,\beta,\zeta) := \{W \in \mathscr{GH}_\infty : \alpha(\omega) < \sigma_i(W(j\omega)) < \beta(\omega), \kappa(W(j\omega)) < \zeta(\omega)\ \forall i,\omega\}$

$$\mathbf{\Pi}(\alpha,\beta,\zeta,\eta) := \{W = \mathrm{diag}\begin{pmatrix} w_1 \\ w_2 \\ \vdots \\ w_p \end{pmatrix} \in \mathscr{GH}_\infty^{p\times p} : \alpha(\omega) < \sigma_i(W(j\omega)) < \beta(\omega), \kappa(W(j\omega)) < \zeta(\omega),$$
$$\left| \frac{d}{d(\log_{10}\omega)} (20\log_{10}|w_i(j\omega)|) \right| < \eta(\omega) \quad \forall \omega, i = 1,2,\ldots,p\}$$

for some given continuous frequency functions $\alpha,\ \beta,\ \zeta,\ \eta : \mathbb{R} \to \mathbb{R}_+$ that satisfy $\beta(\omega) > \alpha(\omega), \zeta(\omega) > 1$ and $\eta(\omega) > 0\ \forall\omega$. For W, α and β delimit the allowable region for its singular values, ζ provides a bound for its condition number and η, expressed in dB/decade, provides bound for the gradient of the magnitude response of its diagonal elements. A^* is the complex conjugate transpose of matrix A. For a given scaled plant $P \in \mathscr{R}^{m\times n}$, further define $\Lambda_{1\omega} = W_1(j\omega)^{-*} W_1(j\omega)^{-1} \in \mathbf{\Lambda_n}$ and $\Lambda_{2\omega} = W_2(j\omega)^* W_2(j\omega) \in \mathbf{\Lambda_m}$.

III. Problem motivation

An important consideration in design is the pole-zero cancelation of modes of lightly damped or undamped plants due to its effects on robust performance and robust stability of the closed-loop system [4]–[8]. Although the algorithm of [2] works well for almost all LTI systems, it does not prevent stable[1] lightly-damped pole-zero cancelations when the shaped plant is formed.

To illustrate this phenomenon, consider a spring-mass system whose transfer function is given as $P(s) = \dfrac{k}{s^2(M_1M_2s^2 + (M_1+M_2)k)}$ [9] based on the measurement of the position of the second mass M_2 as shown in Figure 2(a). This system has a rigid-body mode (M_1 and M_2 in rectilinear motion without friction) and a single vibration mode (spring of stiffness k). Using nominal values of $M_1 = M_2 = 1$Kg and $k = 1\mathrm{Nm}^{-1}$, transfer function of the nominal plant is obtained as $P_0(s) = \dfrac{1}{s^2(s^2+2)}$, i.e. $P_0(s)$ has two undamped poles at $s = \pm j\sqrt{2}$. The algorithm of [2] is now used to synthesize C_∞ and W_1 that shapes the singular values of $P_0(s)$, the singular values of $P_0(s)$ and $P_s(s)$ are shown in Figure 2(b). These plots show that the undamped modes of the nominal plant have been canceled by the synthesized weight. This is undesirable in design as it results in poor robustness of the closed-loop system and is therefore a shortcoming of the algorithm.

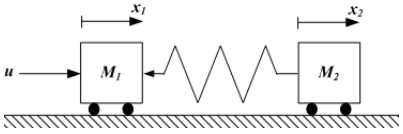

(a) Spring-Mass system

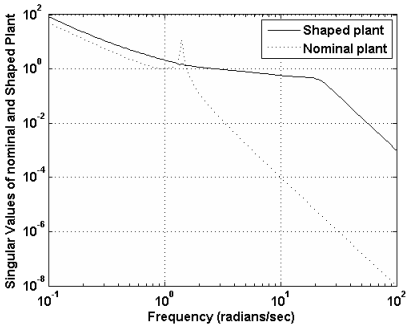

(b) Singular values of P_s and P.

Fig. 2: Schematic diagram of spring-mass system and singular-value plots of P_s and P.

Flexible structures are unique and challenging [10] and the algorithm of [2], when used to design weights for this class of systems, cannot guarantee the avoidance of stable pole-zero cancelations of lightly damped modes as shown above. The aim of this paper is to circumvent this drawback by introducing smoothness constraints on the weights as additional constraints in the weight optimization framework of [2]. The algorithm in this paper is formulated to synthesize only diagonal weights, which is consistent with the observation that diagonal weights are generally sufficient to shape the singular values of a plant [11]. Though with minor modifications as discussed in [2], it is very easy to extend this work also for the synthesis of smooth non-diagonal weights.

IV. Formulation of the smoothness constraints

Here, we describe briefly the weight optimization framework of [2] for the underpinning mathematical machinery of this work. The optimization problem was posed in [2] as follows:

$$\max_{\substack{W_1 \in \mathbf{\Xi}(\underline{w}_1, \overline{w}_1, k_1) \\ W_2 \in \mathbf{\Xi}(\underline{w}_2, \overline{w}_2, k_2)}} b_{opt}(P_s)$$
$$\text{subject to } \underline{s}(\omega) < \sigma_i(P_s) < \overline{s}(\omega)\ \forall i,\omega, \tag{1}$$

where $\underline{s}, \overline{s}, \underline{w}_i, \overline{w}_i$ and k_i $(i = 1,2)$ are continuous real-valued positive frequency functions specified by the designer; $\underline{s}(\omega)$ & $\overline{s}(\omega)$ are the boundaries for an allowable loop-shape. Using the definition of $b(P_s, C_\infty)$ with some algebraic manipulations, optimization problem (1) is massaged into LMI constraints. For brevity, we only state these LMIs when presenting the solution algorithm.

A modification to (1) is now proposed to address the aforementioned drawback by including bounds on the gradients

[1]Note that there is no possibility of unstable pole-zero cancelation using the discussed algorithm since stable minimum phase transfer functions are fitted as loop-shaping weights.

of the magnitude response of the compensators as follows:

$$\max_{\substack{W_1 \in \mathbf{\Pi}(\underline{w}_1, \overline{w}_1, k_1, g_1) \\ W_2 \in \mathbf{\Pi}(\underline{w}_2, \overline{w}_2, k_2, g_2)}} b_{opt}(P_s)$$

$$\text{subject to } \underline{s}(\omega) < \sigma_i(P_s) < \overline{s}(\omega) \ \forall i, \omega, \tag{2}$$

where $\underline{s}, \overline{s}, \underline{w}_i, \overline{w}_i, k_i$ and g_i $(i = 1, 2)$ are continuous real-valued positive functions of the variable ω.

To formulate the smoothness constraint, we consider the magnitude response of the weight and its gradient between two points that are very close to each other. It is intuitive to express this constraint on a log-log scale, i.e. $20\log_{10}|W_i|$ $(i = 1, 2)$ w.r.t. $\log_{10}\omega$, as it is consistent with the notation used in Bode or singular-value plots. For simplicity, denote $\log_{10}\omega$ as ν_ω. We derive constraint for the first diagonal element of the weight, constraints for all diagonal elements are thereafter combined to obtain smoothness constraint for the diagonal MIMO weight in LMI form.

A. Smoothness constraint for W_1

Using the parameterizations earlier given in Section II, where

$$\Lambda_{1\omega} = \text{diag}\begin{pmatrix} \lambda_{1\omega,11} \\ \lambda_{1\omega,22} \\ \vdots \\ \lambda_{1\omega,nn} \end{pmatrix} \text{ and } W_1(j\omega) = \text{diag}\begin{pmatrix} w_{1,11}(j\omega) \\ w_{1,22}(j\omega) \\ \vdots \\ w_{1,nn}(j\omega) \end{pmatrix},$$

we can write for the first diagonal element of W_1, omitting $j\omega$ for concision, as follows:

$$\lambda_{1\omega,11} = |w_{1,11}|^{-2} \Leftrightarrow 10\log_{10}\lambda_{1\omega,11} = -20\log_{10}|w_{1,11}|.$$

Differentiating the above w.r.t. ν_ω, we have

$$\frac{d}{d\nu_\omega}(20\log_{10}|w_{1,11}|) = \frac{d}{d\nu_\omega}(-10\log_{10}\lambda_{1\omega,11})$$

$$= \frac{-10}{\ln 10}\frac{d}{d\nu_\omega}(\ln\lambda_{1\omega,11}) = \left(\frac{-10\lambda_{1\omega,11}^{-1}}{\ln 10}\right)\frac{d\lambda_{1\omega,11}}{d\nu_\omega}. \tag{3}$$

Smoothness constraint for $|w_{1,11}|$ can be stated as

$$\left|\frac{d}{d\nu_\omega}(20\log_{10}|w_{1,11}|)\right| < g_1(\omega).$$

Without loss of generality, we have assumed the same bound on both positive and negative gradients in the formulation via the imposition of the modulus sign. Using (3) on the above, we have

$$\Leftrightarrow \left|\left(\frac{10\lambda_{1\omega,11}^{-1}}{\ln 10}\right)\frac{d\lambda_{1\omega,11}}{d\nu_\omega}\right| < g_1(\omega). \tag{4}$$

$$\Leftrightarrow \left|\frac{d\lambda_{1\omega,11}}{d\nu_\omega}\right| < \frac{\ln 10}{10}\lambda_{1\omega,11}g_1(\omega).$$

Now, considering j-th and $(j-1)$-th grid-points (denoted as ω_j and ω_{j-1}, respectively) which are very close to each other and using differentiation from first principle, we have $\left|\lim_{\nu_{\omega_j}\to\nu_{\omega_{j-1}}} \frac{\lambda_{1\omega_j,11} - \lambda_{1\omega_{j-1},11}}{\nu_{\omega_j} - \nu_{\omega_{j-1}}}\right| < \frac{\ln 10}{10}\lambda_{1\omega_{j-1},11}g_1(\omega_j)$.
Denoting $\nu_{\omega_j} - \nu_{\omega_{j-1}}$ by $\delta\nu$ (assuming constant gridding) and squaring both sides, we have

$$\left(\lambda_{1\omega_j,11} - \lambda_{1\omega_{j-1},11}\right)^2 - \left(\frac{\ln 10}{10}\lambda_{1\omega_{j-1},11}g_1(\omega_j)\,\delta\nu\right)^2 < 0.$$

$$\Leftrightarrow 0 < \left(\frac{\ln 10}{10}\lambda_{1\omega_{j-1},11}g_1(\omega_j)\,\delta\nu\right) - \left(\lambda_{1\omega_j,11} - \lambda_{1\omega_{j-1},11}\right)\times$$
$$\times\left(\frac{\ln 10}{10}\lambda_{1\omega_{j-1},11}g_1(\omega_j)\,\delta\nu\right)^{-1}\left(\lambda_{1\omega_j,11} - \lambda_{1\omega_{j-1},11}\right).$$

Using the above form to express smoothness constraints for the other diagonals and combining the resulting constraints in matrix form, we can then write the smoothness constraint for W_1 as:

$$0 < \left(\frac{\ln 10}{10}\Lambda_{1\omega_{j-1}}g_1(\omega_j)\,\delta\nu\right) - \left(\Lambda_{1\omega_j} - \Lambda_{1\omega_{j-1}}\right)\times$$
$$\times\left(\frac{\ln 10}{10}\Lambda_{1\omega_{j-1}}g_1(\omega_j)\,\delta\nu\right)^{-1}\left(\Lambda_{1\omega_j} - \Lambda_{1\omega_{j-1}}\right), \tag{5}$$

where $\Lambda_{1\omega_j} = \text{diag}\begin{pmatrix} \lambda_{1\omega_j,11} \\ \lambda_{1\omega_j,22} \\ \vdots \\ \lambda_{1\omega_j,nn} \end{pmatrix}$. Using Schur complement lemma [12] on (5), the smoothness constraint for W_1 can be written in LMI form as:

$$\begin{bmatrix} \frac{\ln 10}{10}\Lambda_{1\omega_{j-1}}g_1(\omega_j)\,\delta\nu & \left(\Lambda_{1\omega_j} - \Lambda_{1\omega_{j-1}}\right) \\ \left(\Lambda_{1\omega_j} - \Lambda_{1\omega_{j-1}}\right) & \frac{\ln 10}{10}\Lambda_{1\omega_{j-1}}g_1(\omega_j)\,\delta\nu \end{bmatrix} > 0. \tag{6}$$

B. Smoothness constraint for W_2

Similar to W_1, we consider the first diagonal element of W_2. Based on the parameterizations earlier given, we can write

$$\lambda_{2\omega,11} = |w_{2,11}|^2 \Leftrightarrow 10\log_{10}\lambda_{2\omega,11} = 20\log_{10}|w_{2,11}|$$

Differentiating w.r.t. ν_ω, we have

$$\frac{d}{d\nu_\omega}(20\log_{10}|w_{2,11}|) = 10\frac{d}{d\nu_\omega}(\log_{10}\lambda_{2\omega,11})$$

$$= \left(\frac{10}{\ln 10}\right)\frac{d}{d\nu_\omega}(\ln\lambda_{2\omega,11}) = \left(\frac{10\lambda_{2\omega,11}^{-1}}{\ln 10}\right)\frac{d\lambda_{2\omega,11}}{d\nu_\omega}. \tag{7}$$

In the same manner, smoothness constraint for $|w_{2,11}|$ can be written as

$$\left|\frac{d}{d\nu_\omega}(20\log_{10}|w_{2,11}|)\right| < g_2(\omega).$$

Using the expression in (7) on the above, we have

$$\Leftrightarrow \left|\frac{10\lambda_{2\omega,11}^{-1}}{\ln 10}\frac{d\lambda_{2\omega,11}}{d\nu_\omega}\right| < g_2(\omega).$$

This constraint is in the same form as that formulated for W_1 in (4). Therefore, the combined smoothness constraint for W_2 can similarly be written in LMI framework as follows:

$$\begin{bmatrix} \frac{\ln 10}{10}\Lambda_{2\omega_{j-1}}g_2(\omega_j)\,\delta\nu & \left(\Lambda_{2\omega_j} - \Lambda_{2\omega_{j-1}}\right) \\ \left(\Lambda_{2\omega_j} - \Lambda_{2\omega_{j-1}}\right) & \frac{\ln 10}{10}\Lambda_{2\omega_{j-1}}g_2(\omega_j)\,\delta\nu \end{bmatrix} > 0. \tag{8}$$

Constraints (6) and (8) ensures smoothness in the magnitude response of the compensators point-wise in frequency by restricting the gradient at each frequency grid-point ω_j w.r.t. ω_{j-1} within specified bounds $g_1(\omega_j)$ and $g_2(\omega_j)$, respectively. Hence, these two constraints, in addition to the constraints in [2], yield a complete weight optimization framework for $\mathscr{H}_\infty$ loop-shaping control.

V. Solution algorithm

A sub-optimal algorithm based on the formulation given in Section IV and [2] is now proposed as solution to optimization problem (2). The inputs to the algorithm are (i) a scaled nominal plant $P \in \mathscr{R}^{m\times n}$, where[2] $m \geq n$, (ii) $\underline{s}(\omega)$ and $\overline{s}(\omega)$ which are boundaries for an allowable loop-shape, and for loop-shaping weight W_i $(i = 1,2)$, (iii) $\underline{w}_i(\omega)$ & $\overline{w}_i(\omega)$ that delimit the allowable region for its singular values, (iv) $k_i(\omega)$ that provides bound for its condition number and (v) $g_i(\omega)$ that delimits its gradient. Dropping the dependence on ω_j for $P, C, \underline{s}, \overline{s}, \underline{w}_i, \overline{w}_i, k_i,$ & g_i $(i = 1,2)$ for brevity, the solution algorithm is presented as follows:

1) Find a controller $C_0^\star$ (to initialize the algorithm) such that the interconnection $\left[P, C_0^\star\right]$ is internally stable. Set $i = 0$, where i is the iteration number, and let $\varepsilon^\star_{max,0} = -1$.
2) Increment i by 1.
3) Formulate and solve the following quasiconvex optimization problem at each frequency grid point ω_j, where $j = 1,2,\ldots,N$ and N is selected by the designer[3]:
   Minimize $\gamma^2_{\omega_j}$ such that
   $\exists \Lambda_{1\omega_j} \in \mathbf{\Lambda_n}, \Lambda_{2\omega_j} \in \mathbf{\Lambda_m}$ satisfying
   a) $A^*\mathbf{\Lambda}A \leq \gamma^2_{\omega_j} B^*\mathbf{\Lambda}B$, where $A = \begin{bmatrix} 0 & P \\ 0 & I \end{bmatrix}$, $\mathbf{\Lambda} = \mathrm{diag}\begin{pmatrix} \Lambda_{2\omega_j} \\ \Lambda_{1\omega_j} \end{pmatrix}$ and $B = \begin{bmatrix} I & P \\ C^\star_{i-1} & I \end{bmatrix}$,
   b) $\underline{s}^2\Lambda_{1\omega_j} < P^*\Lambda_{2\omega_j}P < \overline{s}^2\Lambda_{1\omega_j}$,
   c) $\exists \underline{\xi}_{1\omega_j}, \overline{\xi}_{1\omega_j} : \underline{\xi}_{1\omega_j} I < \Lambda_{1\omega_j} < \overline{\xi}_{1\omega_j} I$, $\overline{w}_1^{-2} < \underline{\xi}_{1\omega_j}$, $\overline{\xi}_{1\omega_j} < \underline{w}_1^{-2}$, $\overline{\xi}_{1\omega_j} < k_1^2 \underline{\xi}_{1\omega_j}$,
   d) $\exists \underline{\xi}_{2\omega_j}, \overline{\xi}_{2\omega_j} : \underline{\xi}_{2\omega_j} I < \Lambda_{2\omega_j} < \overline{\xi}_{2\omega_j} I$, $\underline{w}_2^2 < \underline{\xi}_{2\omega_j}$, $\overline{\xi}_{2\omega_j} < \overline{w}_2^2$, $\overline{\xi}_{2\omega_j} < k_2^2 \underline{\xi}_{2\omega_j}$,
   e) $0 < \begin{bmatrix} \frac{\ln 10}{10}\Lambda_{1\omega_{j-1}} g_1\, \delta\nu & \left(\Lambda_{1\omega_j} - \Lambda_{1\omega_{j-1}}\right) \\ \left(\Lambda_{1\omega_j} - \Lambda_{1\omega_{j-1}}\right) & \frac{\ln 10}{10}\Lambda_{1\omega_{j-1}} g_1\, \delta\nu \end{bmatrix}$ when $j > 1$,
   f) $0 < \begin{bmatrix} \frac{\ln 10}{10}\Lambda_{2\omega_{j-1}} g_2\, \delta\nu & \left(\Lambda_{2\omega_j} - \Lambda_{2\omega_{j-1}}\right) \\ \left(\Lambda_{2\omega_j} - \Lambda_{2\omega_{j-1}}\right) & \frac{\ln 10}{10}\Lambda_{2\omega_{j-1}} g_2\, \delta\nu \end{bmatrix}$ when $j > 1$.

   Denote by $\Lambda^\star_{1\omega_j}$ and $\Lambda^\star_{2\omega_j}$ the values of $\Lambda_{1\omega_j}$ and $\Lambda_{2\omega_j}$ $(j = 1,2,\ldots,N)$ that achieve the minimum $\gamma^2_{\omega_j}$ of the optimization problem.
4) Construct *diagonal* transfer function matrices $W^\star_{1,i}(s)$ and $W^\star_{2,i}(s)$ in $\mathscr{GH}_\infty$ by fitting stable minimum phase transfer functions to each magnitude function on the main diagonal of $(\Lambda^\star_{1\omega_j})^{-1/2}$ and $(\Lambda^\star_{2\omega_j})^{1/2}$ $(j = 1,2,\ldots,N)$, respectively.
5) Compute $b_{opt}(W^\star_{2,i}PW^\star_{1,i})$ as detailed in [13] and let this value be denoted by $\varepsilon^\star_{max,i}$. Furthermore, synthesize a controller $C^\star_{\infty,i}$ that achieves a robust stability margin $b(W^\star_{2,i}PW^\star_{1,i}, C^\star_{\infty,i}) = \varepsilon^\star_{max,i}$ usually using the state-space formula given in [14, Theorem 6.3]. Set $C^\star_i = W^\star_{1,i}C^\star_{\infty,i}W^\star_{2,i}$.
6) Evaluate $(\varepsilon^\star_{max,i} - \varepsilon^\star_{max,i-1})$. If this difference (which is always positive) is very small, for instance 0.01, and has remained this small for the last few iterations, then EXIT; otherwise return to Step 2.

The outputs from the algorithm are (i) maximized value of $b_{opt}(P_s)$ obtained in the variable $\varepsilon^\star_{max,i}$, (ii) smooth diagonal loop-shaping weights $W^\star_{1,i}$ and $W^\star_{2,i}$ that achieve $\varepsilon^\star_{max,i}$ and (iii) controller $C^\star_{\infty,i}(s)$ that achieves $b(W^\star_{2,i}PW^\star_{1,i}, C^\star_{\infty,i}) = \varepsilon^\star_{max,i}$.

Being an ascent algorithm, the value of $\varepsilon^\star_{max,i}$ is monotonically non-decreasing as i increases and at each iteration, $\inf_{\omega_j}\left(\frac{1}{\gamma_{\omega_j}}\right) \geq \varepsilon^\star_{max,i-1}$. However, note that the above iterative algorithm cannot guarantee convergence to the global maximum and only monotonicity properties can be guaranteed. The algorithm is quite insensitive to the initial choice of stabilizing controller $C_0^\star$, which is most certainly due to the fact that the algorithm has enough freedom to rectify a poor choice of initial stabilizing controller at both optimization stages 3 and 5 of each iteration.

The quasiconvex problem of Step 3 of the algorithm can be solved using LMI routines. If the robust stability margin is maximized by solving the optimization problem at each frequency ω_j, the initial choice of $\Lambda_{1\omega_j}$ and $\Lambda_{2\omega_j}$ at $\omega_j = \omega_1$ restricts the solution within a cone and can possibly result in unnecessary infeasibility at frequencies corresponding to lightly damped poles/zeros of the plant. However, the LMIs at each frequency ω_j can all be packed together into a single LMI constraint and the optimization problem solved over all frequency grid points in one go to avoid the above difficulty. Circumventing this restriction in this manner inevitably introduces a tradeoff with the available memory and CPU time used to solve the optimization problem.

Remark 1: For optimization over loop-shaping weight W_i $(i = 1,2)$, there are $(m + n + 2i)$ decision variables at each grid-point, i.e. $N(m + n + 2i)$ decision variables $\forall\omega_j$. Hence, the number of decision variables increases as the dimension of the nominal plant increases. Note that the order of the plant does not increase the complexity of the optimization problem since the magnitude value of the plant at each ω_j is used.

VI. Numerical example

We now consider a scaled single-input single-output plant[4] P with lightly damped poles and zeros at $s = -0.0283 \pm j1.4139$ and $s = -0.4 \pm j19.996$, respectively. The transfer function of the scaled nominal plant is

[2] If $m < n$, the dual problem, where $W_1 = W_2^T, W_2 = W_1^T, P = P^T$ and $C_\infty = C_\infty^T$, is easily considered. Hence, there is no loss of generality in imposing this constraint.

[3] The number of grid-points N should be chosen such that the intrinsic properties of the plant and the required performance objectives are adequately captured, for example, if there is lightly-damped pole or zero, then the grid must be sufficiently dense so that the lightly-damped mode is captured.

[4] For simplicity of illustration, a SISO plant is considered and this algorithm can be applied to any MIMO plant without loss of generality as it works efficiently for any $P \in \mathscr{R}^{m\times n}$.

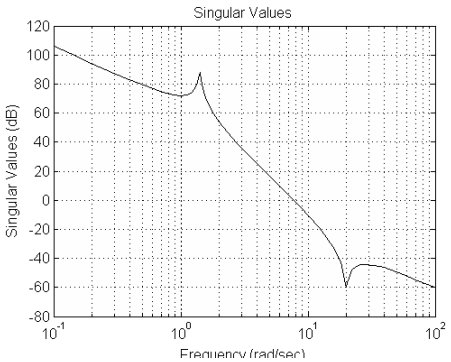

Fig. 3: Singular values of nominal plant

$$P = \frac{10\left(s^2 + 0.8s + 400\right)}{s^2\left(s^2 + 0.0566s + 2\right)} \quad (\zeta = 0.02)$$

and its magnitude plot is shown in Figure 3.

For this plant, loop-shaping weights and $\mathscr{H}_\infty$ loop-shaping controller are to be synthesized such that the desired closed-loop specifications are met via a requirement that the shaped plant lies within the loop-shape boundaries $\underline{s}(\omega)$ and $\overline{s}(\omega)$ given as

$$\underline{s}(\omega) = \frac{\left|\frac{j\omega}{4} + 1\right|}{|j\omega|^2\left|\frac{j\omega}{10} + 1\right|^4} \text{ and } \overline{s}(\omega) = \frac{80\left|\frac{j\omega}{2} + 1\right|^3}{|j\omega|^4\left|\frac{j\omega}{50} + 1\right|},$$

selected based on time-domain specifications. W_2 is fixed at $W_2 = 1$ for simplicity and the solution algorithm formulated in the previous section is then used to simultaneously synthesize W_1 and C_∞. The frequency functions $\underline{w}_1, \overline{w}_1, k_1$ and g_1 that confine the singular values, condition number and the gradient of W_1 are chosen as $10^{-5}, 10^5, 5$ and 80dB/dec, respectively. Note that a different problem specification might require designers selecting more complicated, perhaps frequency dependent bounds.

Two hundred equally spaced frequency grid points between $\omega = 10^{-1}$ and 10^2rad/s on a logarithmic scale are used to formulate the quasiconvex optimization problem in Step 3 and the resulting LMIs are packed into a single optimization problem. Five iterations are required for the practical convergence of the solution algorithm. The singular values of the synthesized W_1, the correspondingly achieved P_s and the simultaneously synthesized C_∞ are shown in Figure 4.

It can be easily seen that the lightly damped poles and zeros of the nominal plant are retained in the shaped plant $P_s = W_2 P W_1$ because the weights are smooth. The shaped plant lies within the specified region denoted by dashed lines and the roll-off rate around cross-over frequency is small as shown in the third figure of Figure 4. Also, W_1 has 8 states with condition number less than 5 at all frequencies, which is typically considered good. As desired, the robust stability margin of 0.5907 is achieved and this indicates a decent design. Also, and more importantly, notice that the gradient of the log-magnitude plot of W_1 with respect to log-frequency is small at every frequency as seen in the second figure of Figure 4. In fact, there is no lightly damped peak in W_1.

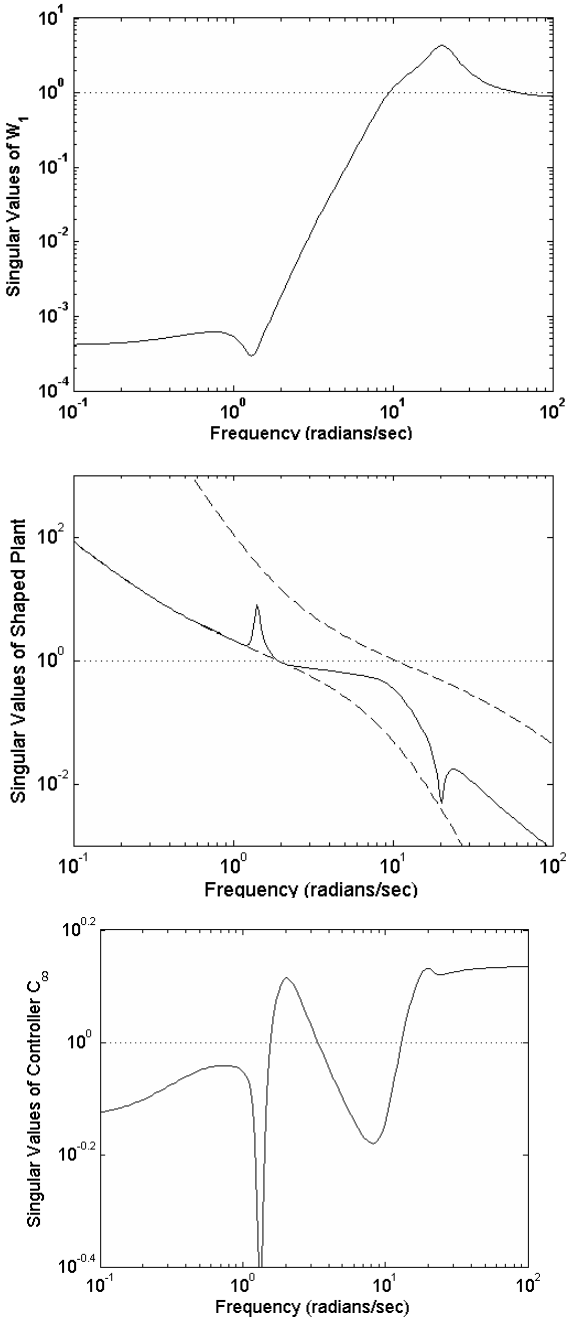

Fig. 4: $\mathscr{H}_\infty$ LSDP with smoothness constraint.

VII. Conclusion

We have formulated smoothness constraints in order to ensure smooth variations in the magnitude response of loop-shaping weights. The constraints are formulated in LMI form and incorporated into a weight optimization framework for $\mathscr{H}_\infty$ loop-shaping control. Smooth weights and a stabilizing controller are consequently synthesized from the resulting solution algorithm. The smoothness constraints limit the gradient of the magnitude response of weights on a log-

log scale thereby preventing pole-zero cancelations of the modes of the nominal plant when the shaped plant is formed. This work therefore extends the applicability of the weight optimization framework to a larger class of LTI systems.

References

[1] D. McFarlane and K. Glover, "A loop-shaping design procedure using $\mathscr{H}_\infty$ synthesis," *IEEE Transactions on Automatic Control*, vol. 37, no. 6, pp. 759–769, 1992.

[2] A. Lanzon, "Weight optimisation in $\mathscr{H}_\infty$ loop-shaping," *Automatica*, vol. 41, no. 1, pp. 1028–1029, 2005.

[3] K. Zhou, J. Doyle, and K. Glover, *Robust and optimal control*. Englewood Cliffs, NJ: Prentice Hall, 1996.

[4] G. Papageorgiou and K. Glover, "A systematic procedure for designing non-diagonal weights to facilitate $\mathscr{H}_\infty$ loop shaping," *Proceedings of IEEE CDC, San Diego, CA, US*, pp. 2127–2132, 1997.

[5] P. Coustal and J. Michelin, "Industrial application of an $\mathscr{H}_\infty$ design method for flexible structures," *Control Systems Magazine, IEEE*, vol. 14, no. 4, pp. 49–54, 1994.

[6] R. Middleton and S. Graebe, "Slow stable open-loop poles: to cancel or not to cancel," *Automatica*, vol. 35, no. 5, pp. 877–886, 1999.

[7] M. Turner and D. Bates, "$\mathscr{H}_\infty$ control design," *Mathematical Methods for Robust and Nonlinear Control:Springer*, 2007.

[8] J. Sikaundi and M. Braae, "Preventing pole-zero cancellation for improved input disturbance rejection in iterative feedback tuning systems," *Novel Algorithms and Techniques In Telecommunications, Automation and Industrial Electronics:Springer*, 2008.

[9] G. Vinnicombe, *Uncertainty and feedback: $\mathscr{H}_\infty$ loop-shaping and v-gap metric*. Imperial College Press, 2001.

[10] A. Preumont, *Vibration control of active structures*, 2nd ed. Kluwer Academic publishers, 2003.

[11] R. Hyde, *$\mathscr{H}_\infty$ aerospace control design-a VSTOL flight application*. In Advances in industrial control series. Berlin: Springer, 1995.

[12] R. Horn and C. Johnson, *Matrix Analysis*. Cambridge University Press, 1996.

[13] K. Glover and D. McFarlane, "Robust stabilization of normalized coprime factor plant descriptions with $\mathscr{H}_\infty$-bounded uncertainty," *IEEE Transactions on Automatic Control*, vol. 34, no. 8, pp. 821–830, 1989.

[14] K. Glover, "All optimal hankel-norm approximations of linear multivariable systems and their $\mathscr{L}_\infty$-error bounds." *International Journal of Control*, vol. 39, no. 6, pp. 1115–1193.